

**DESIGN, OPTIMIZATION AND FABRICATION OF VORTEX
BLADELESS WIND TURBINE**

A Final Year Project Report

Presented to

SCHOOL OF MECHANICAL & MANUFACTURING ENGINEERING

Department of Mechanical Engineering

NUST

ISLAMABAD, PAKISTAN

In Partial Fulfillment
of the Requirements for the Degree of
Bachelor of Mechanical Engineering

By

Muhammad Anas
Muhammad Shehraz Rafiq

June 2022

EXAMINATION COMMITTEE

We hereby recommend that the final year project report prepared under our supervision by:

Muhammad Anas

00000269017

Muhammad Shehraz Rafiq

00000246547

Titled: “Design and Optimization of Vortex Bladeless Wind Turbine” be accepted in partial fulfillment of the requirements for the award of BE MECHANICAL ENGINEERING degree with grade ____

Supervisor: Dr. Sadaqat Ali, Professor SMME, NUST	_____
	Dated: _____
Committee Member: Name, Title (faculty rank) Affiliation	_____
	Dated: _____
Committee Member: Name, Title (faculty rank) Affiliation	_____
	Dated: _____

(Head of Department)

(Date)

COUNTERSIGNED

Dated: _____

(Dean / Principal)

ABSTRACT

Today, energy consumption is much more than energy production. Gone are the days when energy can be produced by carbon emission methods. Researchers have been studying energy harvesting from wind turbines for more than a century, from traditional turbines to the most cutting-edge bladeless turbines. In this project, we designed and optimized a vortex-induced vibrations bladeless wind turbine (BWT). The Vortex bladeless turbine outperforms the traditional wind turbine by taking a completely unique and revolutionary technique to capture wind energy. This device successfully collects the energy of vorticity which is a state of aerodynamic instability. When the wind force is sufficient, the structure begins to vibrate and reaches resonance. It captures wind energy from vorticity phenomena known as the vortex shedding effect. Clearly, bladeless technology consists of a cylinder mounted vertically on an elastic rod, rather than the tower, nacelle and blades which proved to be the essential components of a traditional wind turbine. One of the most essential challenges is to optimize and anticipate produced power, which is one of the most important concerns due to the novelty of this discipline and the extensive investigations across the world. The fluid-solid interactions (FSI) were examined to create a dataset for forecasting techniques in order to improve the generated output electrical power of VBT.

ACKNOWLEDGMENTS

First, we would like to thank Allah Almighty for giving us the courage to keep working on this project in these challenging times. I would like to express my special thanks and gratitude to our teacher as well as our project supervisor, Dr. Sadaqat Ali who gave us the golden opportunity to do this wonderful project on the Bladeless wind turbine. We are obliged for his continuous support and motivation on this project. He always helped us where we were entangled.

TABLE OF CONTENTS

ABSTRACT.....	ii
ACKNOWLEDGMENTS.....	iii
LIST OF TABLES.....	viii
LIST OF FIGURES.....	ix
NOMENCLATURE	xi
CHAPTER 1: INTRODUCTION	1
1.1. Motivation:	1
1.2. Problem Statement:	2
1.3. Objective:.....	3
CHAPTER 2: LITERATURE REVIEW	4
2.1: Aerodynamics:	4
2.2: Lock-in effect.....	5
2.3: Vibration Induced Vibrations:.....	6
2.4: Frequency tuning:.....	6
2.5: Components of Bladeless Wind Turbine:.....	7
2.5.1: Mast:	7

2.5.2: Central Base:.....	8
2.5.3: Alternator:.....	9
2.5.4: Ball and socket joint:	10
2.5.5. Helical Springs:.....	11
2.6: Materials & life span:.....	11
2.7: Cost friendly.....	12
2.8: Different BWT models:.....	13
2.9: Magnetic Arrangement:.....	14
2.9: Literature results.....	17
2.10: Maximum power output.....	19
CHAPTER 3: METHODOLOGY.....	20
3.1. Shaking potential.....	20
3.1.1 Kinetic energy.....	21
3.1.2 Potential energy.....	21
3.1.3 Total energy.....	22
3.2 Accurate Modelling.....	22
3.3 Dynamic modeling:.....	22
3.3.1: Important parameters.....	23

3.3.2: Strouhal number.....	23
3.4 Different models	24
3.4.1: Model 1:.....	24
3.4.2: Model 2:.....	26
3.5: Parts of BWT:	27
3.6: Prepared model of mast:.....	28
3.7: Engineering Design of our model:.....	29
3.8: Material Properties:	30
3.9: Loads and Fixtures:.....	31
3.10: Meshing parameters	32
3.11: Whole structure meshing for fluid analysis:	33
3.12: Final Assembly :.....	35
CHAPTER 4: RESULTS and DISCUSSIONS.....	35
4.1: Theoretical hand Analysis:	35
4.1.1: Wind load:.....	37
4.2: Beam Deflection	38
4.3: Solidworks Analysis:	40
4.3.1: Initial Conditions	40

4.3.2: Size of Computational Domain.....	41
4.3.3: Global Min-Max-Table.....	41
4.4: Solidworks results:	42
4.4.1: Velocity Trajectory in Right plane:	42
4.4.2: Cut Plot Velocity contour:	43
4.4.3: Cut plot Vorticity pattern:	44
4.4.4: Surface plot of vortex:	44
4.5. Reaction Forces:.....	45
4.6. Angular Displacements:	45
4.7. ANSYS Results:.....	46
4.7: Cost Analysis:.....	48
CHAPTER 5: CONCLUSION AND RECOMMENDATION.....	49
5.1: Conclusion:.....	49
5.2: Recommendations:	51
REFERENCES	52
APPENDIX I: Engineering Database	55

LIST OF TABLES

Table 1:Dimensions and properties of the BWT	14
Table 2: Parameters of model 1	25
Table 3: parameters of model 3	26
Table 4: Model properties.....	28
Table 5: Material properties of Rod.....	31
Table 6: Fixed end of rod.....	31
Table 7: Load on rod.....	32
Table 8: Mesh parameters	32
Table 9:Detail mesh information	33
Table 10: Volume of structure	36
Table 11: Desired parameters	37
Table 12: Beam Deflection and Slopes [2]	39
Table 13: Initial conditions	40
Table 14:SW computational domain	41
Table 15:Global Results.....	41

LIST OF FIGURES

Figure 1: Need of renewable energy	2
Figure 2:Electricity trends of Pakistan.....	3
Figure 3: The bladeless wind turbine (a) geometrical model (b) free-body diagram	5
Figure 4:Gerrard’s vortex-formation model	6
Figure 5:positive taper and negative taper mast	8
Figure 6:Central base	9
Figure 7:Alternator.....	10
Figure 8: Ball and socket joint	10
Figure 9: Helical springs.....	11
Figure 10:Production costs	12
Figure 11: (a) BWT1 (b) BWT2 (c) BWT3 (d) BWT4.	13
Figure 12:Circular magnet	15
Figure 13:Bar magnet	16
Figure 14:Radial arrangement.....	16
Figure 15: 3-dimensional magnetic arrangement	16
Figure 16:BWT tip deflection (blue dashed line) and lift force (red line) for (a) BWT1, (b) BWT2, (c) BWT3, (d) BWT4	18

Figure 17:Power level transmitted to BWTs in the lock-in bound	19
Figure 18 : Model 1 of BWT	25
Figure 19: Model 2.....	27
Figure 20: Mast and Rod Engineering Drawing.....	29
Figure 21: Assembly Engineering Drawing	30
Figure 22: Meshed Rod.....	33
Figure 23: mesh Settings.....	34
Figure 24: Computational domain and mesh	34
Figure 25: Application of wind load on base rod	38
Figure 26: Velocity trajectory	42
Figure 27:cut plot velocity contour right plane.....	43
Figure 28:cut plot velocity contour top plane	43
Figure 29:Vorticity pattern	44
Figure 30:Surface plot of vortex	45
Figure 31: Reaction forces vs time	45
Figure 32 : Angular displacement vs time	46
Figure 33:Equivalent (Von-Mises) Stress.....	47

NOMENCLATURE

Net zero	Attain a balance between emissions produced and extracted from atmosphere to decrease the global warming.
VIVACE	vortex-induced vibration aquatic clean energy

CHAPTER 1: INTRODUCTION

1.1. Motivation:

Today we are living in an industrial civilization where energy is the most common need of time. Energy helps in providing a suitable and sustainable life. Energy powers our homes, offices, transportation, and countless other blessings. The population of world is 7.9 billion according to statistics in January 2022.¹ The graph of renewable energy usage is rising around the globe and these alternative energy sources add the keys to combating climate change. According to a survey, 80% of the total energy consumed by humans is derived from fossil fuels. A lot of countries are now looking at wind, solar, hydro, geothermal and many other renewable energy sources because these are the future of our energy resources. Even today, the methods to harness the renewable energy sources is not very efficient, it requires a lot of improvisation and innovation to provide us sufficient energy comparable to fossil fuels. There is a global trend towards a net-zero which bloom the renewable energy production and create a mentality of humans of backing themselves from fossil fuels and leaning on renewable energy sources. Renewable energy is clean and green energy that reduces the greenhouse effect.

¹ <https://www.worldometers.info/world-population/>

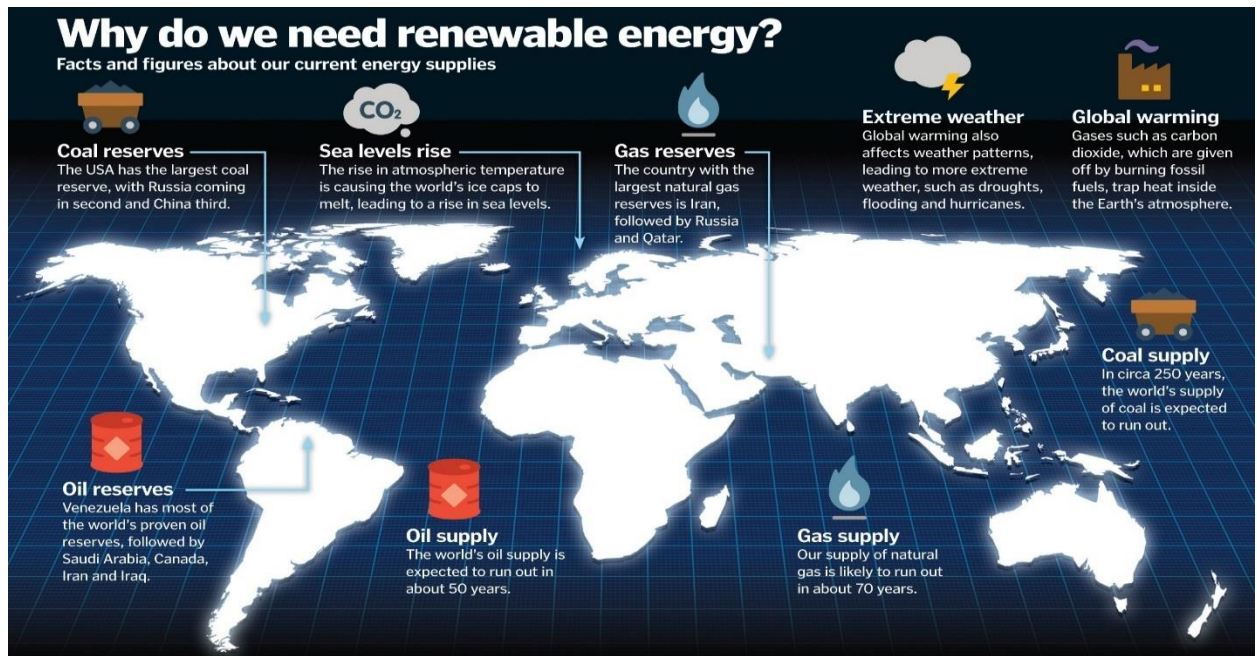


Figure 1: Need of renewable energy

1.2. Problem Statement:

Pakistan is too much relied on the imported fossil fuels which cause a hindrance in the socio-economic progress. This whole scenario leads to substantial increase in fuel prices. According to an article, the gap between energy consumption and demand in Pakistan is 5000 to 8000 MW and this gap is increasing by an average of 7% each year. There is no doubt that Pakistan has abundant renewable energy resources which can contribute a lot in the future energy horizons and provide a Pakistan sturdy base to enhance its economic progress. The purpose of this project is to bring a new source of energy in the market by using a basic engineering phenomenon. Pakistan is facing energy deficit and we want to

lower that deficiency by harnessing the wind power. Wind power is more sustainable than fossil fuels and will reduce the carbon emissions.

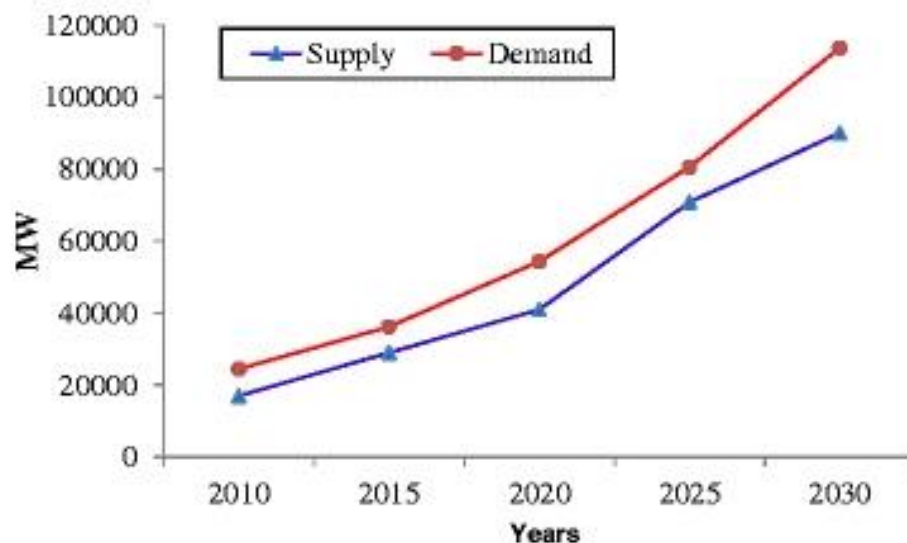


Figure 2:Electricity trends of Pakistan

1.3. Objective:

The main goal of this project is to construct an ecologically sustainable wind turbine with no blades. Horizontal axis wind turbines are basically large blades rotating which cause harm to flying birds. This new technology will be a novel and unique technique to extract wind energy while using few resources and at a reasonable cost. This will generate electricity via a back-and-forth motion of the turbine, and the power generated will be stored for later use. The turbine will generate a large amount of power in a short period of time.

CHAPTER 2: LITERATURE REVIEW

There hasn't been much advancement in this field of inquiry. The different physical phenomena and concepts associated with this field are thoroughly covered. The many issues experienced with traditional windmills are discussed. The use of piezoelectric material to increase the amplitude of oscillation of a vertical windmill is stressed. Diverse words connected to bladeless wind power production are defined, as are numerous types of thread attached to the mast model and various uses. Almost all prior research investigations investigated a VIV harvester comparable to the vortex-induced vibration aquatic clean energy (VIVACE). The VIVACE is a spring-mounted cylinder that generates energy by exhibiting one degree of freedom transverse oscillations at a variety of flow velocities. However, because to the relatively high cost of their supporting framework, VIVACE and comparable devices cannot be readily upscaled. In contrast, a BWT that eliminates the need for linear support by putting the cylinder on the tip of a flexible cantilever. These vortices are often formed near a moving boundary as a result of shear caused by the no slip condition. Vortices, in general, flow with the fluid and are distributed by the viscosity of the fluid.

2.1: Aerodynamics:

Aerodynamic forces are a critical consideration in the design of aero-mechanical structures. Lift and drag forces are the two fundamental aerodynamic forces acting on a body undergoing VIV. Lift forces are desired at low wind speeds because the electricity

produced by the turbine is a function of lift force. A high lift to drag ratio is ideal for the turbine mast design. [1]

(A. Chizfahm, Renewable Energy n.d.)

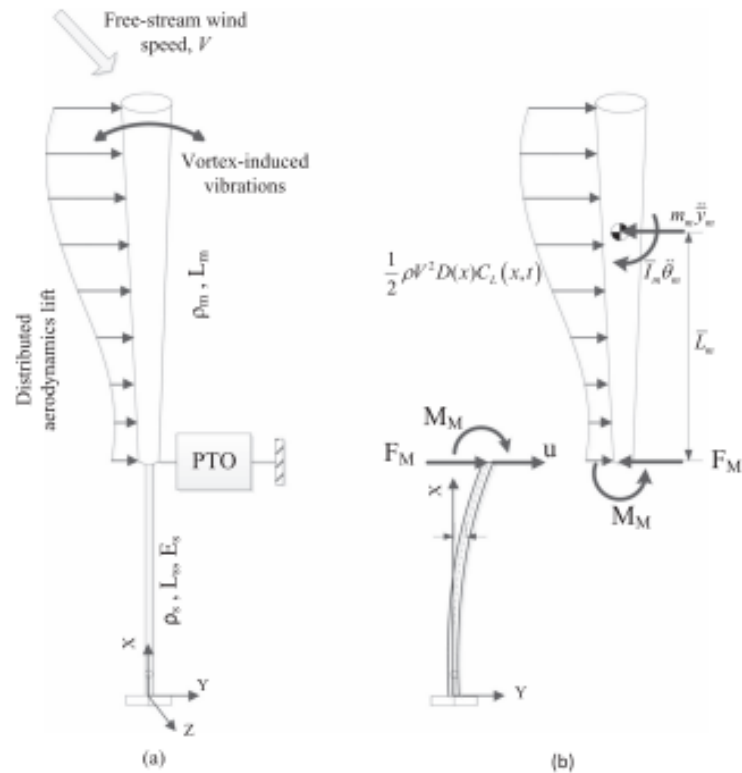


Figure 3: The bladeless wind turbine (a) geometrical model (b) free-body diagram

2.2: Lock-in effect

Lock-in/synchronization/wake-capture is a significant phenomenon connected with bluff body vortex-induced vibrations (VIV). It is distinguished by structural vibrations with a high amplitude. These vibrations can cause fatigue and ultimately to catastrophic structural failure.

2.3: Vibration Induced Vibrations:

When air flows over a body, vortex shedding can cause oscillatory motion. The vortices cause a vibration in the body, which is known as VIV. In VIV, two significant elements are to be emphasized i.e., vortex shedding frequency and vortex wake creation. Karman was the first to propose the production of a wake behind the bluff body. He demonstrated that for an inviscid flow, the optimal arrangement of an infinite double row of vortices is stable for any displacement. Bearman defines a bluff body as one that creates separated flow across a significant fraction of its surface when put in a fluid stream.

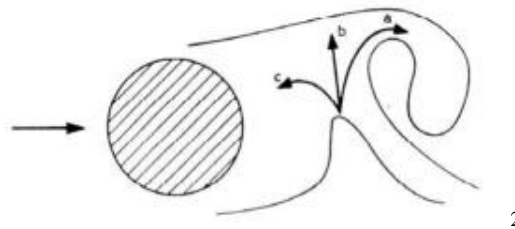


Figure 4:Gerrard's vortex-formation model

2.4: Frequency tuning:

The frequency of Vortex shedding is related to the velocity of the Windstream, although each building has its own unique vibration frequency. To match wind frequencies with a device's natural frequency, among other things, change the body mass (the more

² R Tandel et al 2021 J. Phys.: Conf. Ser. 1950 012058

mass, the less natural frequency) and the stiffness (the greater rigidity, the higher the frequencies). As a result, complicated procedures would be required to adjust the device's inherent frequency. To circumvent this, the Vortex design employs a magnetic confinement system comprised of permanent magnets that enhance the apparent stiffness of the system in proportion to their degree of bending. As the wind strengthens, the degree of bending increases. This is referred to as a "tuning system."

2.5: Components of Bladeless Wind Turbine:

2.5.1: Mast:

It is a straw-like cylindrical or conical construction that is immediately exposed to the upstream wind. Vortex shedding takes place in the wake of the mast. The function of the mast may be tied to the function of the wind turbine blades. The mast must be cylindrical in shape so that the magnitude of vibration is unaffected by wind direction. Furthermore, a modification may be constructed by supplying the cylinder taper, which might be linear or non-linear. Taper ratio is defined as the ratio of cylinder length to the difference between the cylinder's maximum and minimum diameters. Gaster³ carried out water tunnel tests on tapered cylinders with taper ratios of 36:1 and 18:1. When the taper ratio is increased, the attributes such as amplitude and lock in range are nearly comparable

³ Gaster M 1969 Vortex shedding from slender cones at low Reynolds numbers J. Fluid Mech. 38 565–76

to those of a uniform cylinder. The oscillations will not occur if the lowered velocity is not within the lock in range. Taper ratio can be positive or negative, with positive indicating a greater diameter at the bottom and negative indicating a lower diameter at the bottom. In the case of a tapered cylinder, hybrid vortex shedding was found. The point of splitting of 2S and 2P shedding varies throughout the length of the cylinder as the reduced velocity changes from lower reduced velocities at smaller diameter to higher reduced velocities at bigger diameter.

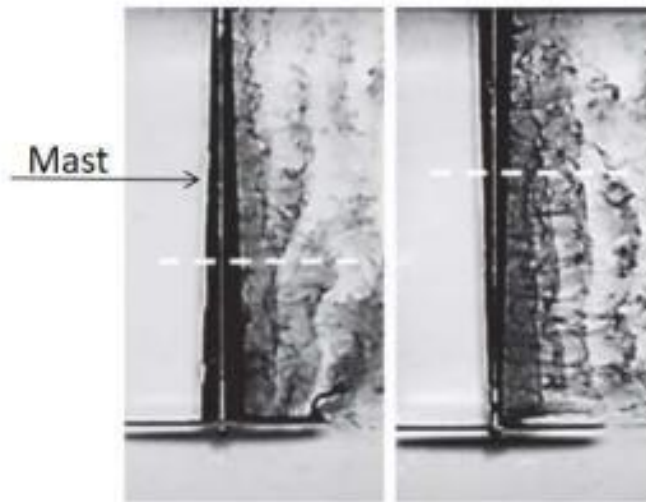


Figure 5: positive taper and negative taper mast

2.5.2: Central Base:

The central base is built of a solid material, such as iron, and serves as the basis for the entire construction. The mast's cantilever motion is supported by a central rod linked to the base. It can also support a variety of electromechanical devices. Because the rod is

subjected to fatigue loading, it must be flexible enough to bend or else the mast's cantilever motion would be hampered. As a result, carbon fibre rod is better suited for this purpose.

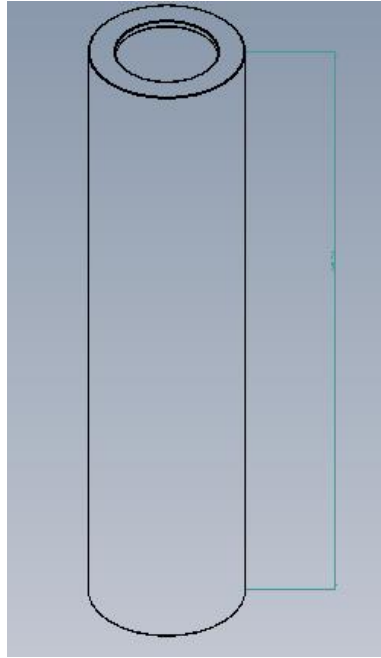


Figure 6: Central base

2.5.3: Alternator:

To convert kinetic energy into electrical energy, electromagnetic devices relate to oscillatory motion of the mast or cantilever action of the rod. Because of the increased energy loss in piezoelectric devices, electromagnetic devices are favored. One significant consideration is that the orientation or operation of these devices should not be affected by wind direction. Similarly, an alternator with a ring-shaped magnet on the mast acts as a

rotor, while the stator on the rod is unaffected by wind direction. Electrostatic devices, such as variable capacitors, can be utilized in addition to piezo and electromagnetism.



Figure 7: Alternator

2.5.4: Ball and socket joint:

Ball-and-socket joints are triaxial joints that allow rotation about three axes. A ball and socket joint is a type of coupling consisting of a ball-shaped part that fits into a ball-shaped socket.

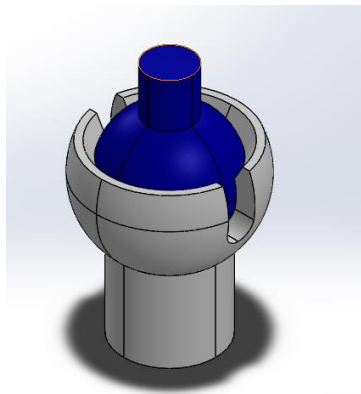


Figure 8: Ball and socket joint

2.5.5. Helical Springs:

Helical springs can be manufactured to absorb, eject, twist, or maintain a compressive, tensile, or torque force or energy between surfaces. Once the potential energy from the spring is released, the elastic coil returns to its original helical-shaped form.

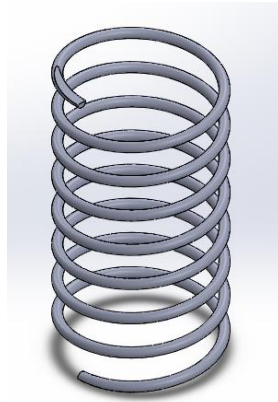


Figure 9: Helical springs

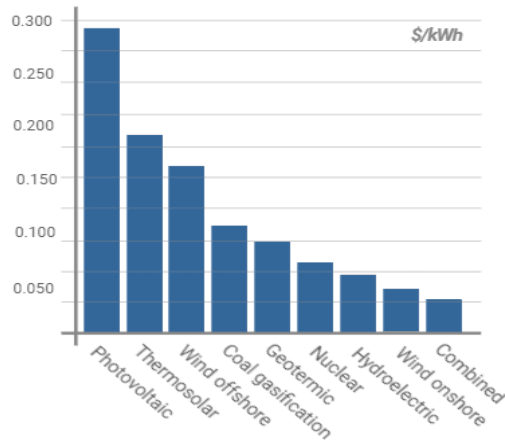
2.6: Materials & life span:

Current wind turbine technology must withstand a wide range of load levels at varying wind speeds, putting severe mechanical demands on transmission components such as gears, bearings, bushings, and brakes. The numerous moving parts are continually worn, resulting in substantial maintenance expenses. Wind turbines with no blades eliminate any mechanical pieces that might wear out due to friction. Carbon fiber polymers, plastics, steel, neodymium, and copper are the primary materials utilized in the production

of Vortex turbines. These materials' operating limitations are significantly beyond Vortex's operational norms.

2.7: Cost friendly

The cheap costs connected with Vortex turbines are one of their key advantages. The levelized cost of energy (LCOE) of Vortex turbines will be lower, allowing for a faster return on investment. As a result, this technology is very competitive not just against generations of alternative or renewable energy, but also against conventional technologies. Research on the cost-effectiveness of bladeless turbines may be found here. These cost savings are the result of creative design and raw material use. There is no need for a nacelle, support systems, or blades, which are often expensive components in traditional wind turbines.



(Bladeless n.d.)

Figure 10: Production costs

2.8: Different BWT models:

The VIV bladeless wind turbines consist of a relatively long cylinder that is either flexible or mounted on a flexible structure exposed to air flow.

BWT1: A right circular flexible cylinder

BWT2: A conic flexible cylinder

BWT3: A right circular rigid cylinder mounted on a flexible beam

BWT4: A conic rigid cylinder mounted on a flexible beam

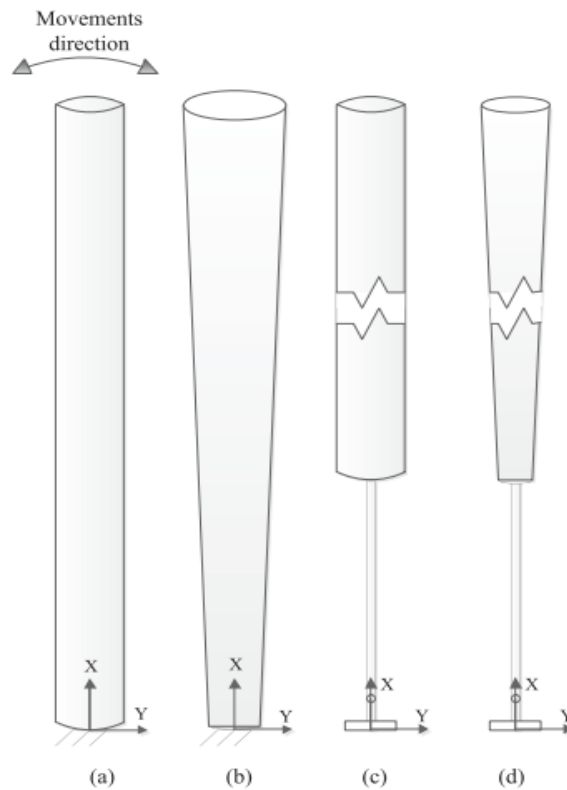


Figure 11: (a) BWT1 (b) BWT2 (c) BWT3 (d) BWT4.

Table 1:Dimensions and properties of the BWT

(A. Chizfahm, Dynamic modeling of vortex induced vibration wind turbines 2018)

Physical Properties	BWT1	BWT2	BWT3	BWT4
Lengths (L_m, L_s) (m)	(4,0)	(4,0)	(4, 0.15)	(4, 0.15)
Mean diameter of the mast D (m)	0.18	0.225	0.375	0.375
Mast thickness t (m)	0.001	0.001	0.001	0.001
Stand diameter D_s (mm)	–	–	0.018	0.018
Mass density (ρ_m, ρ_s) ($\times 10^3$ kg/m ³)	(1.04,0)	(1.04,0)	(1.04, 8)	(1.04, 8)
Mass (m_m, m_s) (kg)	(2.6,0)	(4.4,0)	(5.21,0.39)	(5.27,0.39)
Young's modulus E_s (GPa)	2.2	2.2	2.2	2.2
Taper ratio c	–	2	–	2

2.9: Magnetic Arrangement:

Various design possibilities for electromechanical conversion systems in bladeless wind turbines are investigated. The effect of variations in the magnetic field system's shape, size, and configuration on the generated voltage is analyzed. Mast oscillates perpendicular to wind direction. When the mast body vibrates, it cuts the magnetic field lines and hence a voltage is induced in the coils based on Faraday's laws of electromagnetic induction. According to this law, an EMF is induced across a coil when the flux linkage through the coil changes with time. If N is the number of turns in the coil and ϕ be the flux linked to the coil, then emf (E) generated would be given as

$$E = -N(d\phi/dt)$$

As wind can have any direction, we cannot use linear alternator. We must design a system that caters for all directions (360°). Following models were observed.

- A ring magnet with the coils (on mast body) placed in the middle of the ring has the advantage of being symmetric in all directions (Figure 10)
- Bar magnets in circular fashion around mast (Figure 11)
- Radial arrangement of bar magnets around mast (Figure 12)
- A 3-dimensional magnetic arrangement is proposed where at-least three sets of two bar magnets are used. It is a multilayered 3D structure with 6 bar-magnets. (Figure 13)

For all the arrangement studied, flux is minimum(negligible) at the center (mast body) except for the last one where magnets are stacked in layers with specified angles. When the two magnets were kept at 145° , the flux change was found to be maximum and hence this will generate more emf across the coils for a given vibration

The following features in the magnetic field system of bladeless wind turbines would generate maximum voltage for a given wind speed in any direction.

- Three layers of 2-pole bar magnets
- All the layers are placed at 120° apart with N-N structure
- Each layer has 2 bar magnets placed at 145°
- Depending on cost and space, bar magnets of highest surface area and more length are preferred.

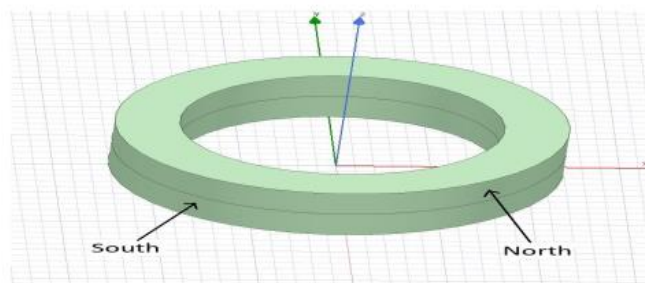


Figure 12: Circular magnet

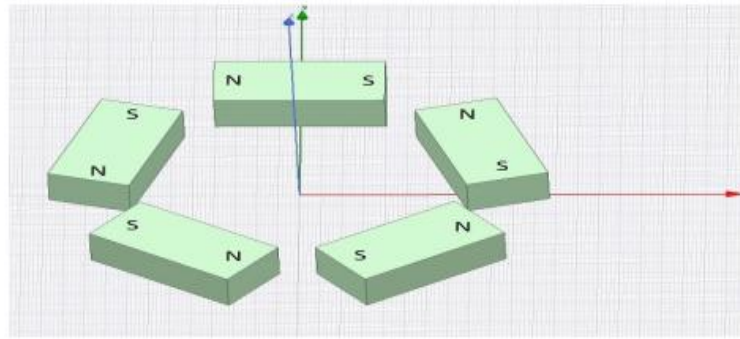


Figure 13: Bar magnet

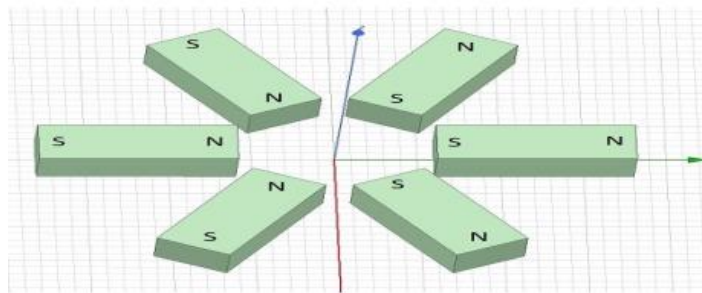


Figure 14: Radial arrangement

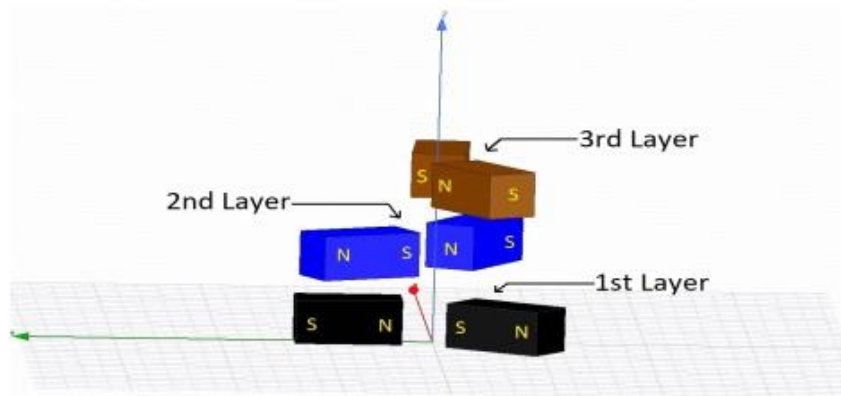


Figure 15: 3-dimensional magnetic arrangement

2.9: Literature results

The power level supplied to BWTs and analyze fluctuations in the level as a function of free-stream velocity to compare suggested configurations fairly, the features of BWTs are chosen to attain equivalent dynamic characteristics in all BWTs. Because lock-in is the most significant dynamic characteristic of a BWT, all BWTs are intended to experience lock-in around the air speed of 4.3m/s. Since the top end has a high frontal area and a long moment arm, the flow produces a dominating resultant moment at the vortex shedding frequency and, as a result, bigger deflections. Large deflections improve vortex shedding and boost lift force. However, at low air speeds, the lock-in occurs at the lower end of the turbine, which, due to its short frontal area and moment arm, cannot create a dominating moment at the lock-in frequency. In BWT1, on the other hand, the vortex shedding frequencies of all parts along the height are the same, and therefore the lift force of all sections is in the same frequency. The lift force comprises a single significant frequency component that amplifies the forced vibrations at low air velocity. Because of the conical form of BWT4, it has a greater moment of inertia than a BWT3 with the same mean diameter. As a result, as compared to BWT3, BWT4 has a lower natural frequency, which facilitates the lock-in phenomena at lower air speed.

(A. Chizfahm, Dynamic modeling of vortex induced vibration wind turbines 2018)

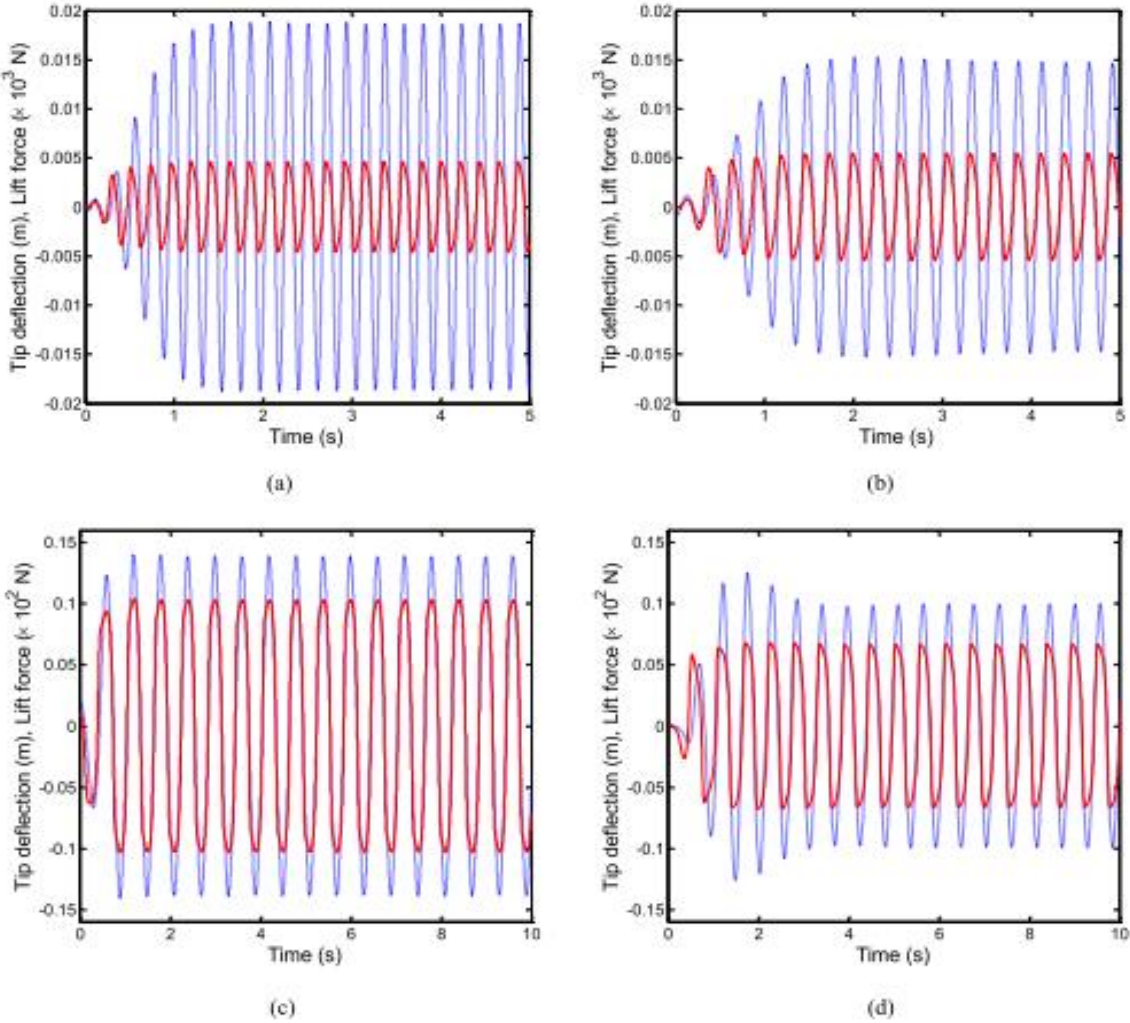


Figure 16: BWT tip deflection (blue dashed line) and lift force (red line) for (a) BWT1, (b) BWT2, (c) BWT3, (d) BWT4

2.10: Maximum power output

The amplitudes of the vibrations of the BWTs increased when the vortex shedding frequency matched the natural frequency of the structure, which is known as the lock-in phenomenon. Furthermore, the simulation findings showed that conic BWTs work better in the post-synchronization zone (i.e., high wind speeds), but right circular cylinder BWTs perform better in the pre-synchronization region (i.e., low wind speeds). It was also proved that mounting the bluff body on a flexible framework leads in a considerable increase in power transferred to the BWT when compared to employing a flexible bluff body. the natural frequencies and the mode shapes are different due to the nonuniform diameter of the structure.

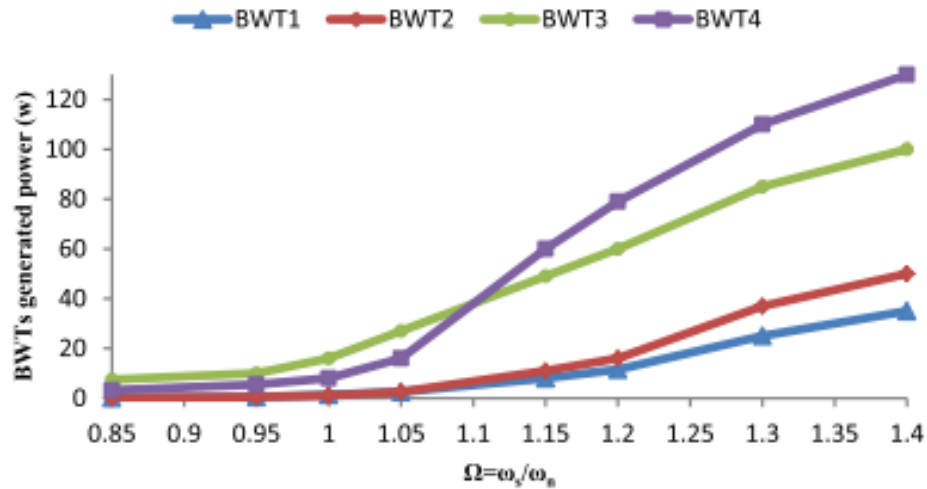


Figure 17: Power level transmitted to BWTs in the lock-in bound

CHAPTER 3: METHODOLOGY

This bladeless wind turbine (BWT) is based on vortex-induced vibration which occurs when shedding vortices, a von Karman vortex street phenomenon exert oscillatory lift forces on a body perpendicular to flow direction. It forms a cylindrical shape that moves perpendicular to the wind flow and generates power through linear motion. To sustain the motion required to create energy, this is known as the property of oscillation. The produced electricity will then be sent to a battery bank, where it will be stored.

3.1. Shaking potential

A simple harmonic motion is the release of an object's reciprocating motion. The movement, or oscillating motion, is a type of vibration. That to-and-fro motion cause the system to exhibit the simple harmonic motion and possess the shaking force. Mechanical oscillations around an equilibrium point are referred to as vibrations. The equation of motions for SHM is

$$F = -k x$$

where F denotes the force of harmonic motion, x is the displacement of the oscillating body from its equilibrium position, and k denotes the spring constant for a mass on a spring.

$$m a = -k x$$

$$a = - (k/m) x$$

$$d^2x/ dt^2 = -(k/m) x$$

where m is the mass of the cylindrical body, and t is time in seconds by which it oscillates. By using our knowledge of mechanical vibrations and differential equations course, solving the differential equation above, a solution which is a sinusoidal function is obtained.

$$x(t) = c_1 \cos \omega t + c_2 \sin \omega t = A \cos (\omega t - \phi)$$

where c_1 and c_2 are two constants defined by the initial circumstances and the origin is assumed to be the equilibrium position, ‘‘A’’ is the amplitude, ω is the angular frequency, and ϕ is the phase angle which is zero if the waves are in-phase and it is 180 degrees if the waves are out-of-phase.

3.1.1 Kinetic energy

The kinetic energy possessed by our bladeless wind turbine due to vibration induced by the winds and vortex produced is given by

$$KE = 1/2 mv^2 = kA^2 \sin^2 (\omega t - \phi)/2$$

3.1.2 Potential energy

The potential energy stored in our bladeless wind turbine is mainly due to its stiffness and the displacement from its mean position. this potential energy is mainly elastic potential energy which is expressed as

$$PE = 1/2 kx^2 = kA^2 \cos^2 (\omega t - \phi)/2$$

3.1.3 Total energy

The total energy in our project is the summation of potential and kinetic energies due to wind velocity and the stiffness of our structure.

$$\text{Total energy} = \text{KE} + \text{PE} = 1/2 kA^2$$

3.2 Accurate Modelling

A model for the forced-vibrations of the structure subjected to fluid flow forces obtained by the Navier-Stokes equations in the presence of moving boundaries is required for an accurate model of VIV bladeless wind turbines. The numerical model, however, is ineffective for structural design and controller synthesis due to its computational complexity. Furthermore, computational challenges exist when modelling three-dimensional (3D) flexible VIV wind turbines with huge aspect ratios.

3.3 Dynamic modeling:

The dynamic modelling of the mast is equivalent to that of a cylindrical bluff body and is accomplished using a numerical approach and a FEM analysis in software such as Ansys and Solidworks. Many researchers have created dynamic models of bluff bodies over the last few decades, including free and forced vibration models, lowering damping models, and nonlinear exciters.

3.3.1: Important parameters

Bladeless wind turbine is accurately modelled by examining fluid flow over a body using the Navier-Stokes equation in the presence of a moving body. During dynamic modelling, two things are calculated i.e., lift force and tip deflection at various wind speeds.

The lift force is proportional to the body's cross-sectional area. A larger cross-sectional area produces more lift force, resulting in a faster wind speed. Synchronization happens at lock in range in the case of BWT, which is the optimal state. In the case of a tapered mast, a smaller diameter area produces more lift force during the pre-synchronization period, i.e., at a lower velocity than the lock in velocity. A bigger diameter area produces more lift force during the post-synchronization period, i.e., at a higher velocity than the lock in velocity. In the case of a cylindrical mast, the cross-sectional area remains constant along its length. As a result, the lift force on a cylindrical pole stays constant along its length. So, during the pre-synchronized phase, the right circular cylinder will provide more power, whereas the tapered or conical mast will provide more power during the post-synchronized phase.

3.3.2: Strouhal number

The Strouhal Number is a measure of the ratio of inertial forces owing to flow unsteadiness or local acceleration to inertial forces due to changes in velocity from one place in the flow field to another.

$$St = \frac{fD}{U}$$

where, f is the frequency of vortex shedding, D is characteristics length or diameter of the bluff body and U is fluid stream velocity.

$$f = st \frac{U}{L} = 0.2 \times \frac{6}{0.206} = 5.825 \text{ Hz}$$

3.4 Different models

We prepared two types of models with different dimensions to find out the best model. There are 2 shapes of BWT which we assigned as Model 1 and Model 2.

3.4.1: Model 1:

This model is made in Solidworks by using a straight cylinder without any taper. The cylinder is made hollow to lower its weight and increase the oscillations. The strand rod is attached with the mast and is oscillating with the mast body.



Figure 18 : Model 1 of BWT

Table 2: Parameters of model 1

Design Name	Total height(mm)	Total Diameter(mm)
1.1	4000	500
1.2	5000	600
1.3	2500	450
1.4	2700	450

3.4.2: Model 2:

This model is made in Solidworks by using a straight cylinder using taper. The cylinder is made hollow to lower its weight and increase the oscillations. The strand rod is attached with the mast and is oscillating with the mast body. The mast's conical form facilitates the lock-in phenomena across a larger range of wind speeds. When the wind strikes the mast, it vibrates owing to the vortices that create as well as the spring placed at the bottom of the mast. During oscillation, the energy absorbed raises the amplitude. Depending on the direction of the wind, one thread is pulled from the mast's rib during the back-and-forth motion of the mast.

Table 3: parameters of model 3

Design Name	Total height(mm)	Total Diameter(mm)	Taper Ratio
2.1	4000	500	1.5
2.2	5000	600	1.5
2.3	2500	450	2
2.4	2700	450	2



Figure 19: Model 2

3.5: Parts of BWT:

The BWT structure has three main parts that are fixed together:

1. Cylindrical mast made of glass fiber.
2. Flexible rod made of reinforced carbon fiber that is fixed to mast
3. Special cover that anchors the carbon fiber rod to the foundation

3.6: Prepared model of mast:

After taking into consideration the average yearly velocity is 5 m/s in Islamabad.

According to this data vortex turbine is designed. Considering the notations as follows

D_{\min} = lower diameter of mast

D_{\max} = upper diameter of mast

D = mean diameter

d = rod diameter

L_1 = length of mast

L_2 = total length of rod

t = thickness of mast

U = average air velocity

Table 4: Model properties

Sr. No.	Parameters	Dimensions (mm)
1	D_{\min}	105
2	D_{\max}	200
3	d	25
4	L_1	2000
5	L_2	2700
6	t	6

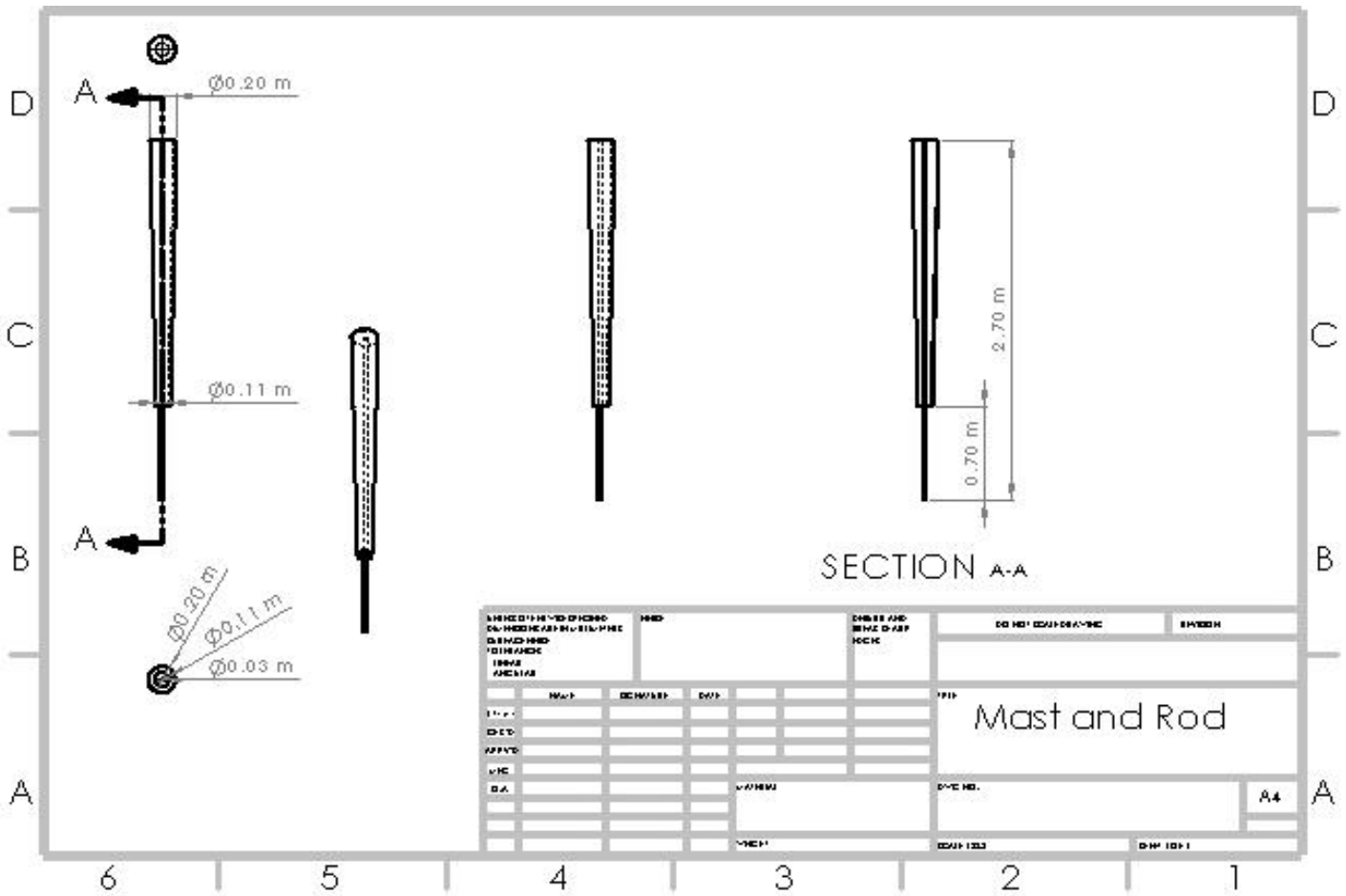


Figure 20: Mast and Rod Engineering Drawing

3.7: Engineering Design of our model:

We prepared the design model of our analysis on the Solidworks. We first created the part of mast, rod, and base of the structure. Then we created this assembly by using mate feature. The next part was to import this assembly into drawing format. There are different views of this assembly which will help the reader to understand.

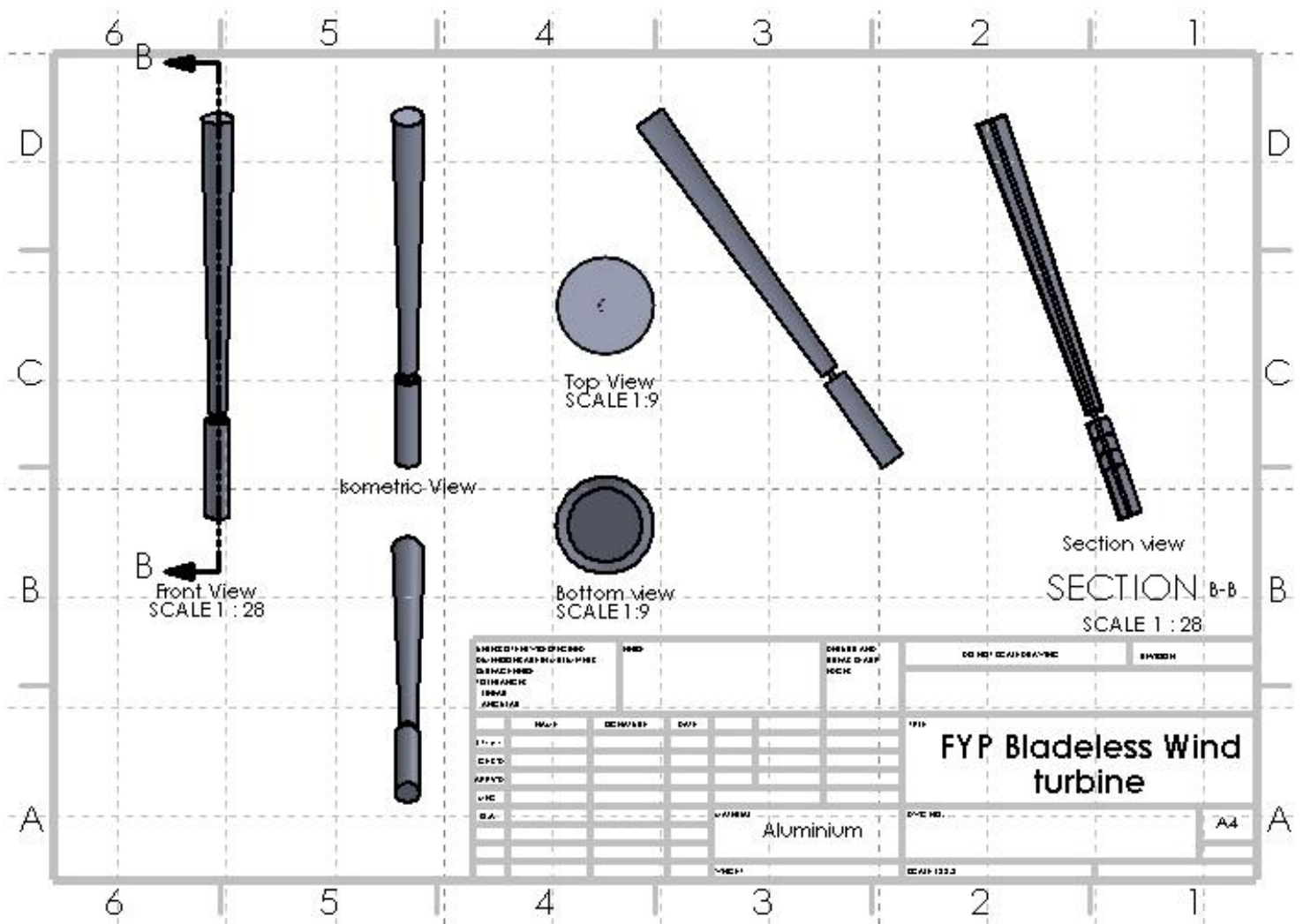


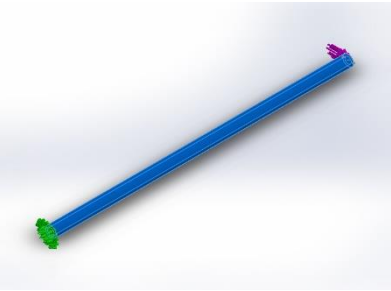
Figure 21: Assembly Engineering Drawing

3.8: Material Properties:

We used SolidWorks to do analysis of shear stress and Von misses stress and find the value of deflection in the rod which we used. The rod is attached with mast, and it is

the point at which different stresses and failure can occur. The material which we use for analysis of rod is 1060 Aluminum Alloy.

Table 5: Material properties of Rod

Model Reference	Properties	Components
	Name: 1060 Alloy Model type: Linear Elastic Isotropic Default failure criterion: Max von Mises Stress Yield strength: 2.75742e+07 N/m² Tensile strength: 6.89356e+07 N/m²	Solid Body 1(Boss-Extrude1)

3.9: Loads and Fixtures:

The lower end of the rod is attached with a fixed support on the ground. we plan to constrain this end via using concrete plate. this fixed end sure no displacement in any direction and is shown as a fixed geometry in the table.

Table 6: Fixed end of rod

Fixture name	Fixture Image	Fixture Details
Fixed-1		Entities: 1 face(s) Type: Fixed Geometry

The wind profile will cause a distributed loading on the rod, and we just found the values of that force in SolidWorks analysis which is equal to 6.125 Newton.

Table 7: Load on rod

Load name	Load Image	Load Details
Force-1		Entities: 1 face(s), 1 plane(s) Reference: Right Plane Type: Apply force Values: 6.125 N

3.10: Meshing parameters

Your high-quality mesh in SolidWorks to simulate this rod. this road has no transition of length, so we turned off the automatic transition.

Table 8: Mesh parameters

Mesh type	Solid Mesh
Mesher Used:	Standard mesh
Automatic Transition:	Off
Include Mesh Auto Loops:	Off
Jacobian points for High quality mesh	16 Points
Element Size	6.0377 mm
Tolerance	0.301885 mm
Mesh Quality	High

Model name: Part1
Study name: SimulationXpress Study(-Default-)
Mesh type: Solid Mesh

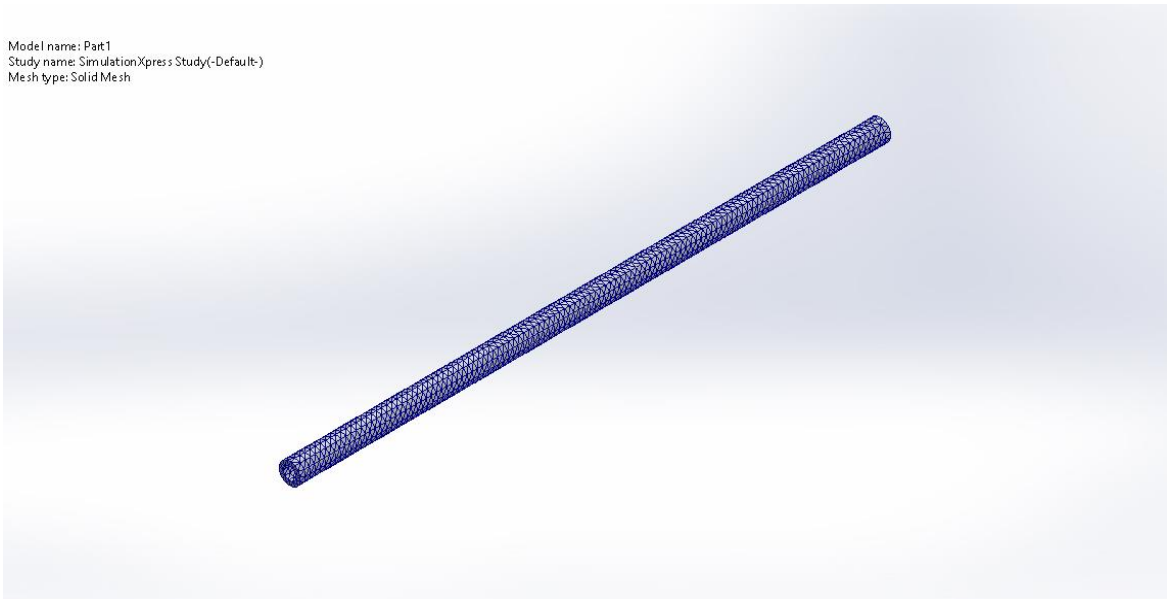


Figure 22: Meshed Rod

Table 9:Detail mesh information

Total Nodes	15243
Total Elements	7720
Maximum Aspect Ratio	3.9697
% Of elements with Aspect Ratio < 3	99.7
Percentage of elements with Aspect Ratio > 10	0
Percentage of distorted elements	0
Time to complete mesh(hh:mm:ss):	00:00:02

3.11: Whole structure meshing for fluid analysis:

The mast and rod structure are meshed in SolidWorks to conduct the fluid analysis. the mesh settings are set on 4 on the scale of 1-7. the computational domain is a rectangular geometry which will show the fluid contained inside this geometry.

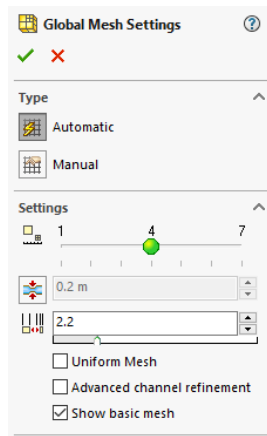


Figure 23: mesh Settings

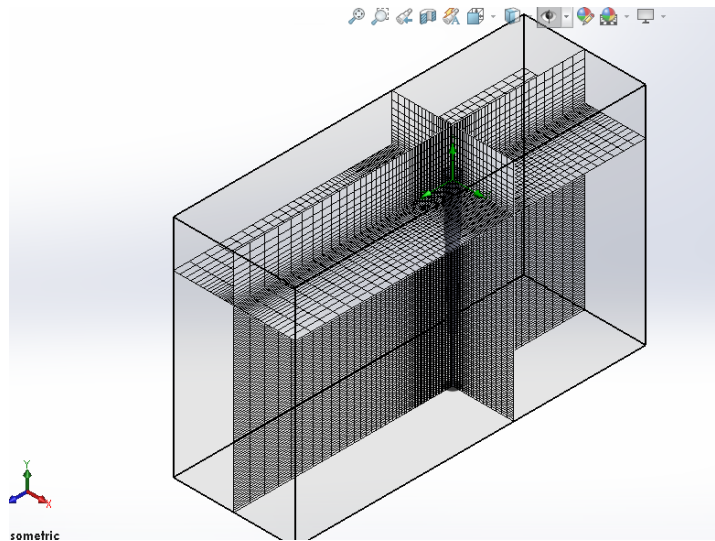
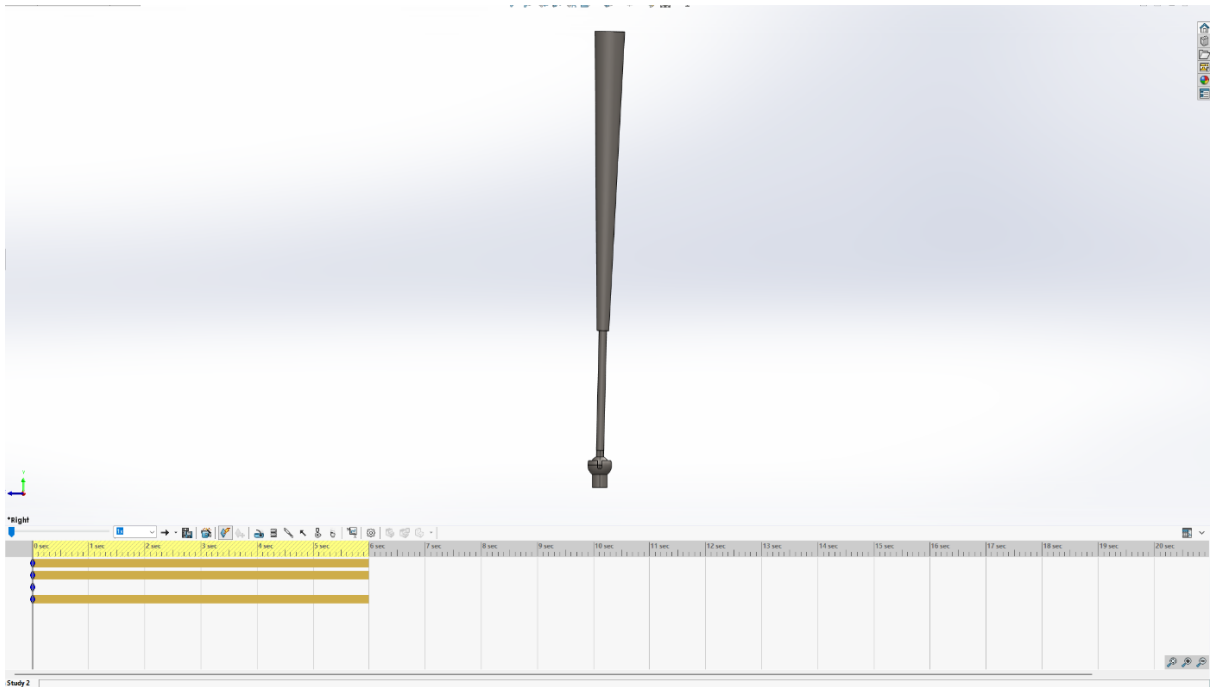


Figure 24: Computational domain and mesh

3.12: Final Assembly :



CHAPTER 4: RESULTS AND DISCUSSIONS

The primary goal of this study is to analyze the performance of power production, we consider simulated settings near to the lock-in zone with a free air speed of 5 m/s.

4.1: Theoretical hand Analysis:

We did theoretical hand analysis on our model and used the engineering knowledge to find the values of different parameters.

$$\text{Volume of truncated cone} = \frac{\pi h}{3} \times (R^2 + Rr + r^2)$$

$$\text{volume of cylinder/disc} = \pi r^2 h$$

volume of shell(Mast);

$$= \frac{2\pi}{3} [\{.1^2 + (.1)(.0525) + .0525^2\} - \{.094^2 + (.094)(.0465) + .0465^2\}] + \pi(0.006)(.094^2 - .0075^2) + \pi(0.006)(.0465^2 - .0075^2) = 0.005728 \text{ m}^3$$

$$\text{volume of Rod} = \pi(2.7)\{.0125^2 - .0075^2\} = 0.000848 \text{ m}^3$$

Table 10: Volume of structure

Sr. No	Parameter	Value
1	Volume of mast	0.005728 m ³
2	Volume of rod	0.000848m ³

$$\text{Total volume of System(including rod and mast)} = 0.006576 \text{ m}^3$$

$$\text{density of Aluminium} = 2710 \text{ kg/m}^3$$

$$\text{Modulus of Elasticity of Aluminium} = E = 68 \text{ GPa}$$

$$\text{mass of Aluminium} = \rho v = 2710 \times 0.006576 = 17.82 \text{ kg}$$

$$\text{Moment of Inertia} = I = \frac{\pi}{64} (.025^4 - .015^4) = 1.668 \times 10^{-8} \text{ m}^4$$

$$\text{stiffness of rod} = k = \frac{3EI}{L^3} = \frac{3 \times 6.8 \times 10^9 \times 1.668 \times 10^{-8}}{0.7^3} = 9920.467 \frac{\text{N}}{\text{m}}$$

$$\text{natural frequency of rod} = \omega = \sqrt{k/m} = 18.217 \text{ rad/sec}$$

Table 11: Desired parameters

Sr. No	Parameters	Values
1	Total volume of System	0.006576 m^3
2	density of Aluminum	2710 kg/m^3
3	mass of aluminum	17.82 kg
4	Moment of Inertia	$1.668 \times 10^{-8} \text{ m}^3$
5	stiffness of rod	$9920.467 \frac{\text{N}}{\text{m}}$
6	<i>natural frequency of rod</i>	18.217 rad/sec

4.1.1: Wind load:

Force exerted by wind on the structure is calculated by; [1]

$$F = PAC_D$$

$$A = 0.305 \text{ m}^2$$

$$P = 0.613 V^2 = 22.068 \text{ Pa}$$

$$\frac{L}{D} = 13.11 \quad [2]$$

C_D for circular section corresponding to 13.11 is 0.91

$$F = 6.125 \text{ N}$$

$$\omega = 2\pi(5.825) = 36.60 \text{ rad/sec}$$

4.2: Beam Deflection

Assuming that all the bending takes place in rod, no bending within mast. So, our point of interest is rod, the wind load can be represented at the top of rod

$$\sum F_x = 0; \quad F = V = 6.125 \frac{m}{s}$$

$$\sum M = 0; \quad M = F \times L = 4.2875 \text{ N m}$$

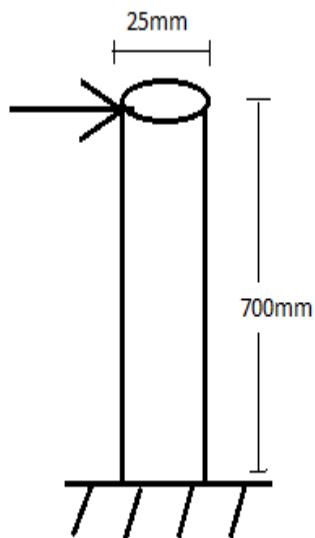


Figure 25: Application of wind load on base rod

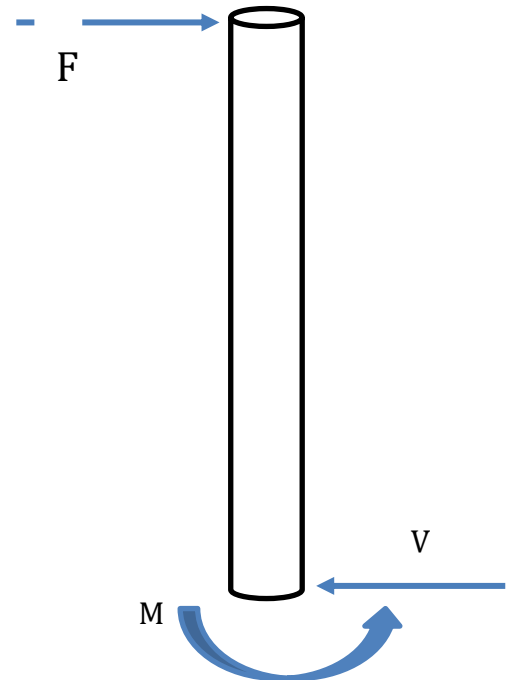
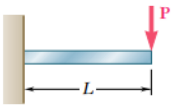
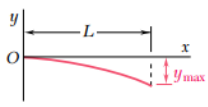


Figure 20: FBD of rod

Table 12: Beam Deflection and Slopes [2]

Beam and Loading	Elastic Curve	Maximum Deflection	Slope at End	Equation of Elastic Curve
		$-\frac{PL^3}{3EI}$	$-\frac{PL^2}{2EI}$	$y = \frac{P}{6EI}(x^3 - 3Lx^2)$

$$\text{Max Deflection} = \delta = \frac{FL^3}{3EI} = 0.617\text{mm}$$

For a cylinder of Diameter 25mm, Y_{\max} is 12.5mm

$$\text{Max Stress} = \sigma = Y_{\max} \frac{FL}{I} = 3.213\text{MPa}$$

$$\text{Slope} = \theta = \frac{PL^2}{2EI} = 0.001323$$

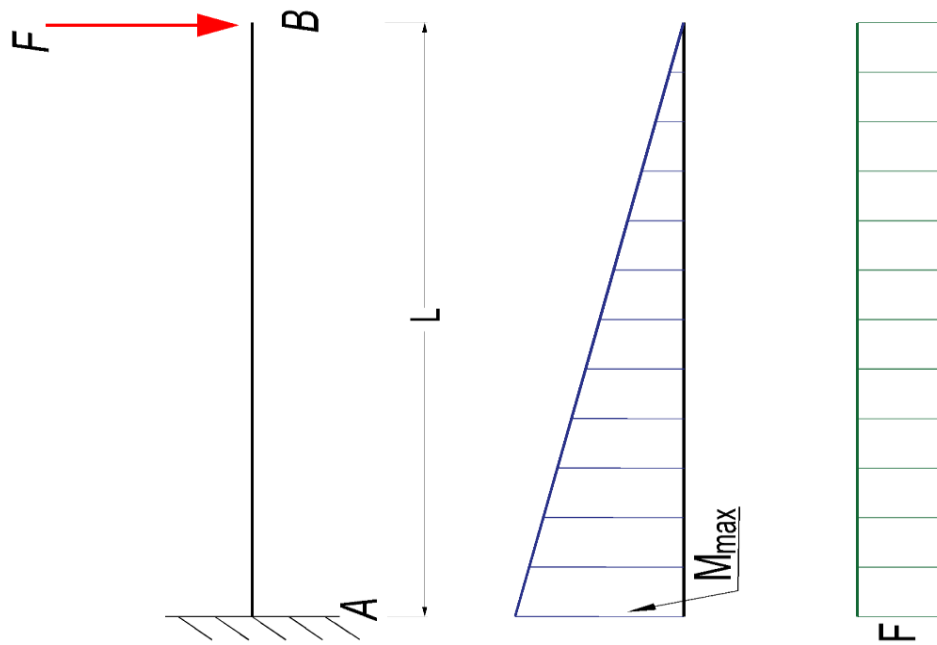


Figure 21: Moment and Shear force behavior

4.3: Solidworks Analysis:

4.3.1: Initial Conditions

Table 13: Initial conditions

Thermodynamic parameters	Static Pressure: 101325.00 Pa Temperature: 293.20 K
Velocity parameters	Velocity in X direction: 0 m/s Velocity in Y direction: 0 m/s Velocity in Z direction: 5.000 m/s

4.3.2: Size of Computational Domain

Table 14:SW computational domain

X min	-0.887 m
X max	0.898 m
Y min	-2.617 m
Y max	0.686 m
Z min	-1.934 m
Z max	3.206 m

4.3.3: Global Min-Max-Table

Table 15:Global Results

Name	Minimum	Maximum
Pressure [Pa]	101298.52	101349.20
Temperature [K]	293.18	293.21
Velocity [m/s]	0	7.901
Mach Number []	0	0.02
Vorticity [1/s]	2.97e-05	478.09
Relative Pressure [Pa]	-26.48	24.20
Shear Stress [Pa]	0	0.35
Bottleneck Number []	1.9162924e-18	1.0000000

Acoustic Power [W/m ³]	1.126e-62	9.885e-10
Acoustic Power Level [dB]	0	29.95

4.4: Solidworks results:

We carried out results in Solidworks and find the followings:

4.4.1: Velocity Trajectory in Right plane:

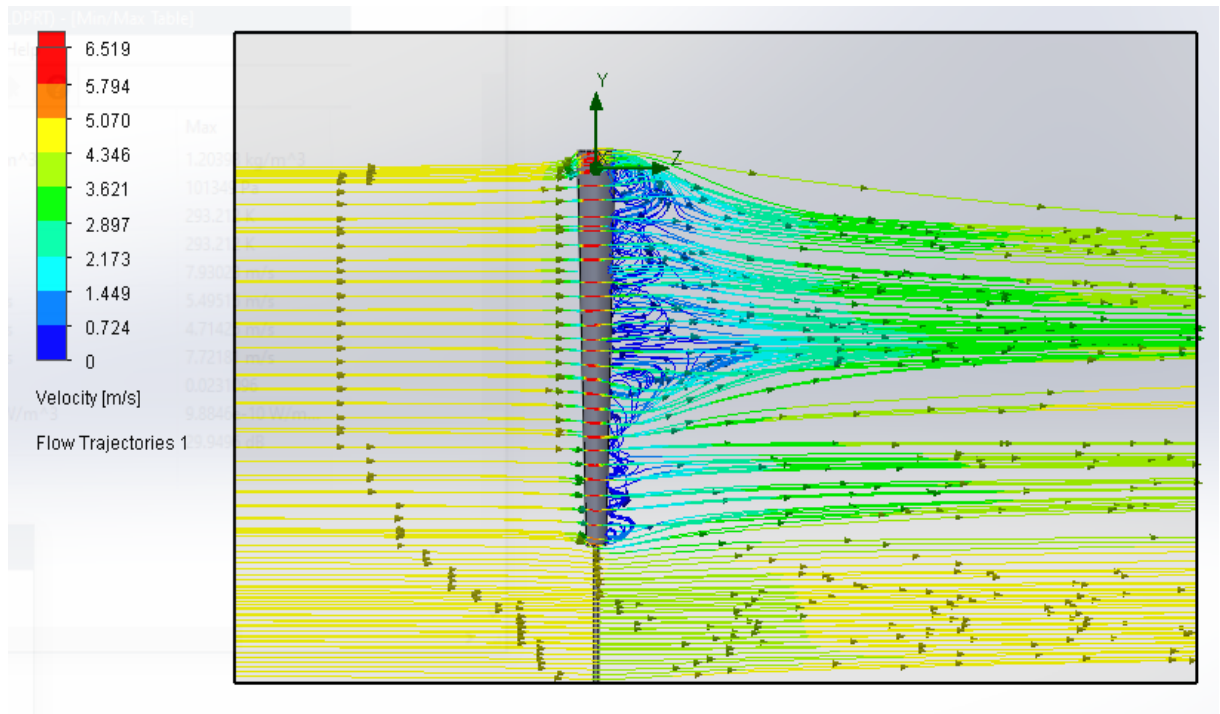


Figure 26: Velocity trajectory

Here the wind is flowing in the positive z-axis and the legend shows the maximum and minimum velocity regions. This trajectory is more fascinating while watching in animation.

4.4.2: Cut Plot Velocity contour:

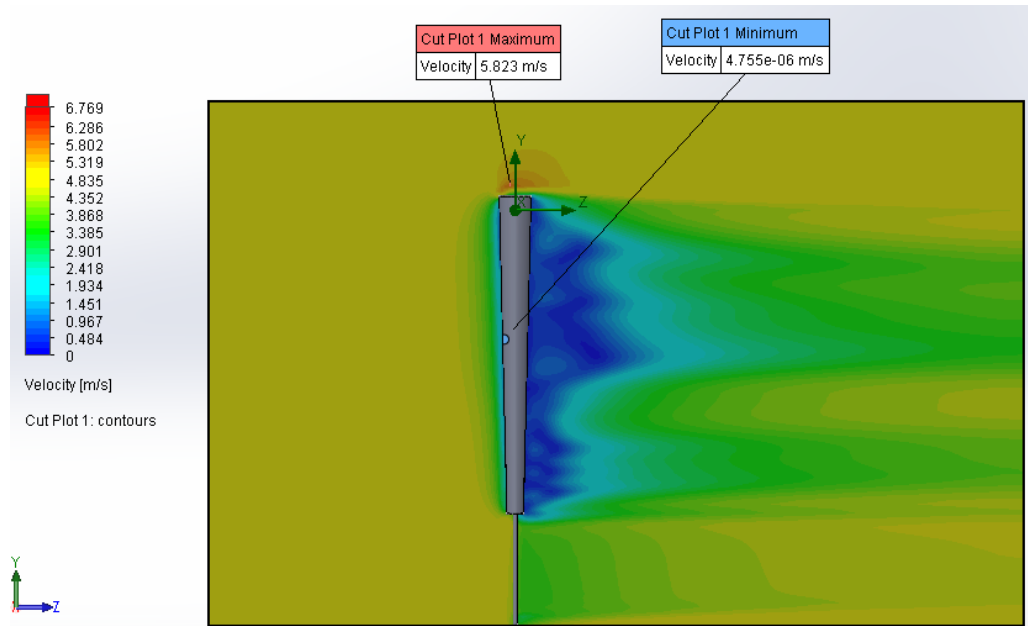


Figure 27:cut plot velocity contour right plane

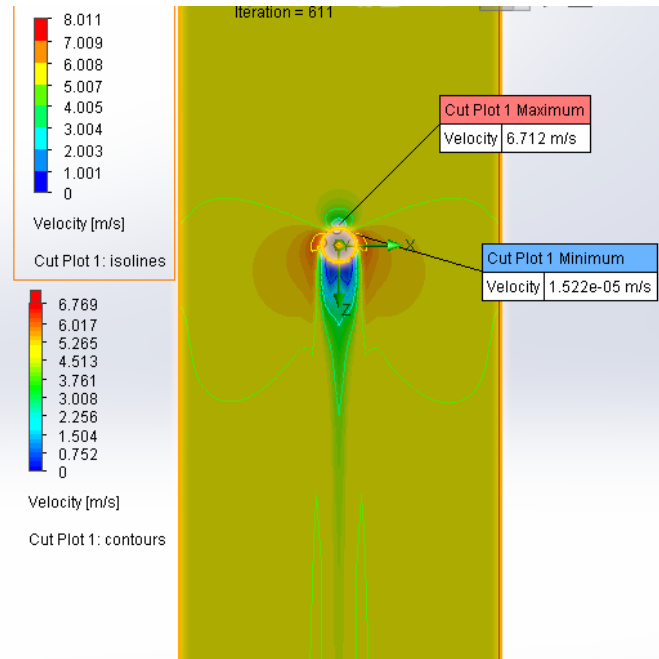


Figure 28:cut plot velocity contour top plane

4.4.3: Cut plot Vorticity pattern:

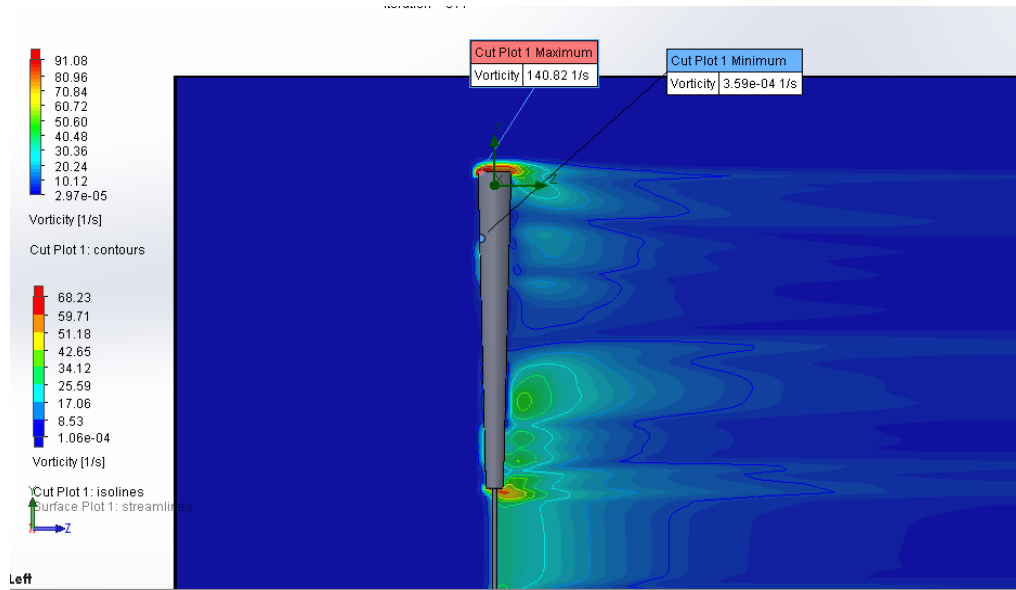


Figure 29: Vorticity pattern

4.4.4: Surface plot of vortex:

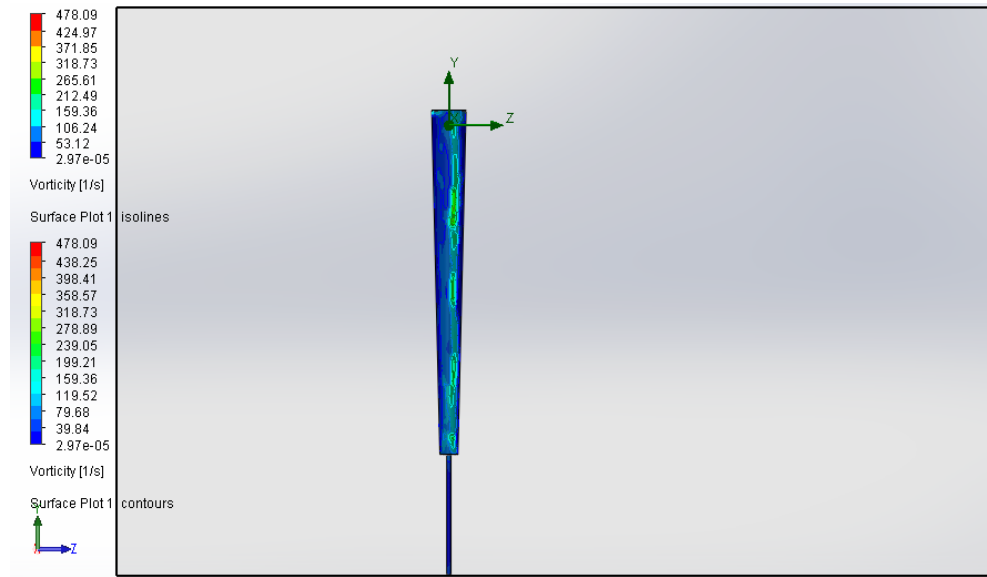


Figure 30:Surface plot of vortex

4.5. Reaction Forces:

In SolidWorks, we did the analysis of reaction forces against time. The graph shows a sinusoidal waveform which varies to 612 N.

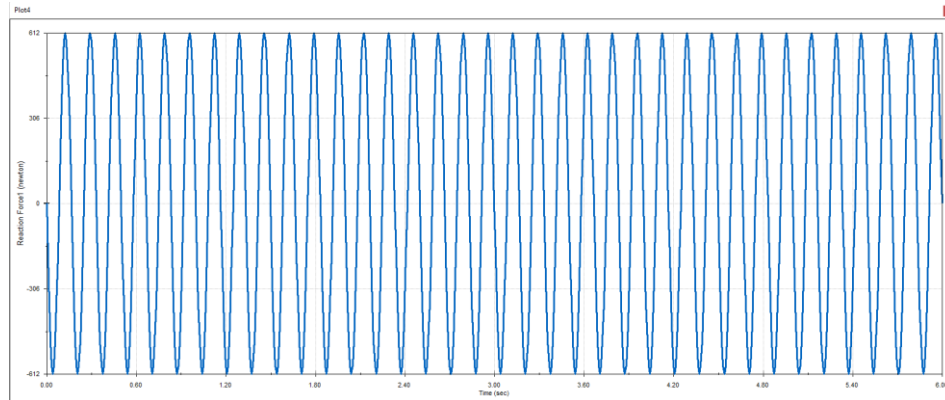


Figure 31: Reaction forces vs time

4.6. Angular Displacements:

We kept the base stationary and found the angular displacement in Solidworks with reference to the top of the structure.

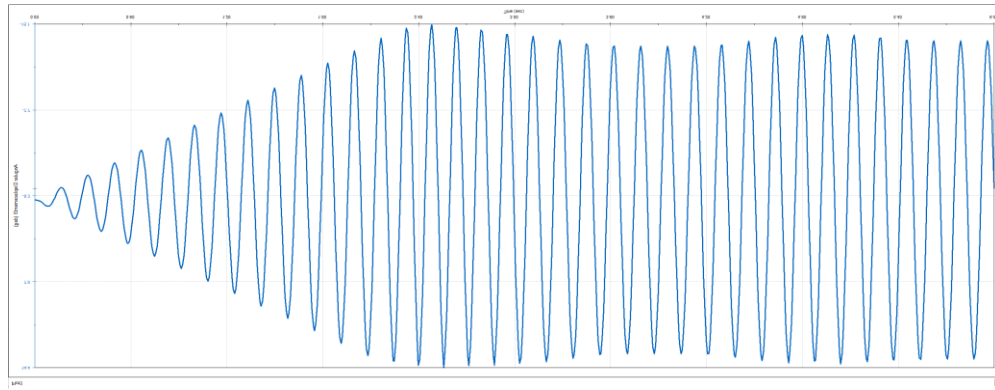


Figure 32 : Angular displacement vs time

4.7.ANSYS Results:

ANSYS is used to do analysis on our system. Following parameters were calculated using ANSYS static structural,

- Equivalent (Von-Mises) Stress
- Total Deformation

The maximum value of stress of $2.5773e6$ at the circumference of base rod. Which is obvious that the stress is maximum at the farthest point from mean position. The minimum value of stress is found at the center of the rod which is $82.043e5$. as we move radially from center to outward of rod the stress increases. The maximum stress generated is way less than the elastic limit of aluminum. So, our material is not going to fail at this stress. We have not yet studied the behavior of turbine at higher velocities. Therefore, we cannot say anything about the stress at higher velocities.

The maximum deformation of 3.7553mm is produced by the rod. That is at the top of mast. Our magnet arrangement is around base, so we are not interested in that rather we are interested in the deflection of rod. The rod deflection from ANSYS at the height of 600mm from ground is 0.41726mm. this is very little deflection. Due to very little deflection in the rod, we cannot harvest the energy of this system

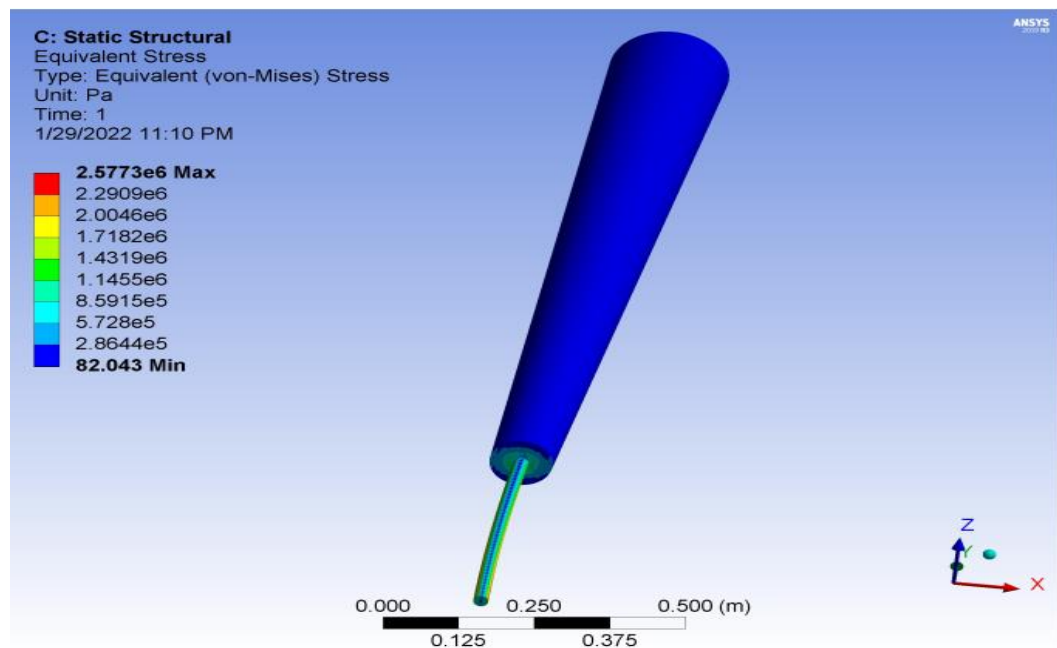


Figure 33:Equivalent (Von-Mises) Stress

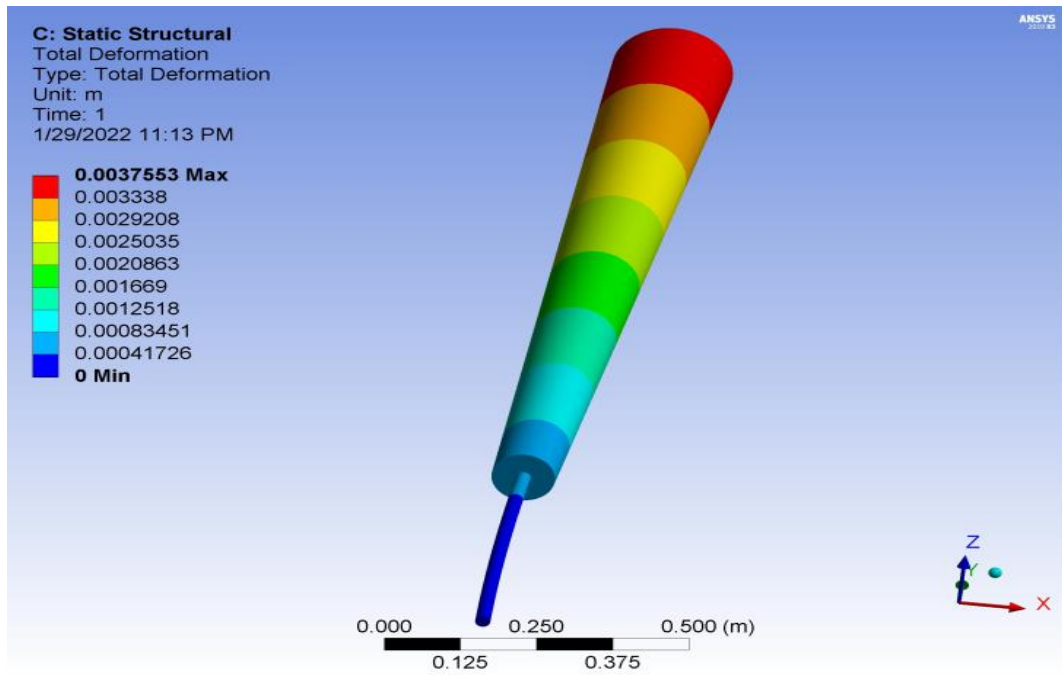


Figure 34: total Deformation

4.7: Cost Analysis:

Initial carbon fiber was selected as our primary material due to its light weight and high strength [4]. Upon doing detailed analysis on aluminum, Steel and Carbon Fiber; we chose Aluminum.

Material	Cost per kg (\$)	Elastic Modulus (GPa)
Carbon fiber	22	250
Steel	1.7	190
Aluminum	3.1	68

Among these materials Aluminum is the stiffer. We cannot use carbon fiber with these properties because it has very high stiffness. Either we have to make composite of using carbon fiber and other materials or chose another. Cost of alone structure was 82 USD which is not acceptable. Keeping in mind the stiffness and cost, Aluminum is chosen as our working material. Though we could perform more analysis on material, but we are not only focusing of material.

The mass of Aluminum used is 17.82 *kg*. Additional Aluminum for base would be roughly take the total required mass to 25kg.

Cost of 1kg Aluminum = 3.1 USD

Cost of 25kg Aluminum = 77.5 USD

Cost of 1 small rectangular neodymium magnet is 6 USD [5]. Total of 6 magnets are going to be used. So total cost of magnets will be 36 USD. Other wiring and energy conversion and storage devices would cost roughly around 20 USD.

The estimated cost of a 2.7m tall turbine is 140 USD.

CHAPTER 5: CONCLUSION AND RECOMMENDATION

5.1: Conclusion:

In this era of rising global warming, reducing CO₂ emissions as quickly as possible is critical to humanity's survival. Wind power has the potential to be a superior choice for

generating sustainable power without emitting CO₂. Power generation through vortices of wind have advantages over other energy sources, few of those are enlisted below.

- Absence of gears, bearings, and lubricants
- Environment friendly
- Can be combined with solar panels
- Can be installed on highways (due to its working principal)
- Occupies less space as compared to conventional wind turbines

This technology is still in its early stages of development and has a long way to go. It takes a lot of intelligence to combine electromagnetism and fluid dynamics in this way. Conventional rectifying, filtering and electrical regulation methods are equally applicable as expected. As on other alternators electric power output is AC with variable amplitude and frequency. After rectification and filtering it is transformed into DC.

We chose the best design available to conduct analysis, but it is still not enough to generate power. Material change, design and magnetic arrangement changes are needed to be observed in order to progress in Bladeless wind turbine. By changing the shape of the turbine, hybrid vortex shedding can be done to get maximum output.

Lift and Drag coefficients are to be adjusted such a way that maximum energy from wind can be extracted. This can be done by not taking approximate values instead exact values should be found and used to get better results.

Resonance occurs for a short period of time; we have to make sure that the structural frequency is in range with the average wind vortex frequency so maximum energy can be

harvested. This means we have to change parameters of structure according to different regions to compensate for the vortex frequency i.e., as the average wind speed changes, the structure needs to be optimized.

5.2: Recommendations:

A lot of research has been done on this technology over last decade but unfortunately a practical bladeless wind turbine has not been brought into market. It shows how complex it is while designing and considering other parameters to make this turbine work.

- Different materials with the appropriate strength and stiffness can be found to lighten the system, and different layouts can be tested to lower the natural frequency.
- Exact moment of inertia of tapered conic shell can give better results
- Efficient mechanisms can be developed to convert the structural energy into electrical energy.
- It is necessary to consider the environmental parameters at installation sites, as operating conditions may not always be suitable for turbine operation.
- Making the central rod hollow could increase the deflection and ultimately power generation.

REFERENCES

- [1] E Azadi Yazdi 2018 Smart Mater. Struct. 27 075005. Nonlinear model predictive control of a vortex induced vibrations bladeless wind turbine.
- [2] Fluid Mechanics: Fundamentals and Applications Book by John Cimbala and Yunus A Çengel (2004), Table 11-2.
- [3] Mechanics of Materials, 8th Edition by Ferdinand Beer and E. Johnston and John DeWolf and David Mazurek, Appendix D.
- [4] VIV resonant wind generators, David Jesús Yáñez Villarreal, Vortex Bladeless S.L. www.vortexbladeless.com
- [5] cost of neodymium magnet, <https://www.magnetshop.com/neodymium-magnet>
- [6] Gaurao Gohate, Abhilash Khairkar, Sameer Jadhav, Study of vortex induced vibrations for harvesting energy, Int. J. Innov. Res. Sci. Technol. 2 (11) (2016) 374–378.
- [7] O. Rishabh, B. Shubhankar, S.K. Vishal, Bladeless wind power generation, Int. J. Sci. Eng. Dev. Res. 2 (4) (2017) 163–167.
- [8] B. Seyed-Aghazadeh, D.W. Carlson, Y. Modarres-Sadeghi, The influence of taper ratio on vortex induced vibration of tapered cylinders in the cross flow direction, J. Fluids Struct. 53 (2015) 84–95.
- [9] Cajas JC, Houzeaux G, Yanez DJ, Mier-Torrecilla M. SHAPE Project Vortex ~ Bladeless: Parallel Multi-code Coupling for Fluid-structure Interaction in Wind Energy Generation

- [10] R. Gabbai, Benaroya, H, ‘An overview of modeling and experiments of vortex-induced vibration of circular cylinders’, *Journal of Sound and Vibration*, 2005, 282.3, pp. 575-616.
- [11] W. Graebel, ‘Advanced fluid mechanics’, Academic Press, 2007.
- [12] Ayhan Demirbas & Murad I. Andejany (2017) Optimization of wind power generation using shaking energy, *Energy Sources, Part B: Economics, Planning, and Policy*, 12:4, 326-331, DOI: 10.1080/15567249.2015.1112860
- [13] Adeyanjuand Boucher; *JSRR*, 26(10): 93-106, 2020; Article no.JSRR.63908
- [14] SarpkayaT.Vortex-InducedOscillations.*JournalofAppliedMechanics*.1979;241-258
- [15]Lin,Zhonglu.NumericalStudyoftheInteractionbetweenFluidandMultipleCylinders.Firs
tYearReport.2016;179.6
- [16].LienhardJohnH.UniversityofHoustonResearch.UniversityofHoustonWebsite;1966.Ja
nuary1.AccessedOctober24,2019.
- [17] D.J.Y. Villarreal, VIV resonant wind generators, www.vortexbladeless.com, June 7th (2018)
- [18] Akaydin H D, Elvin N and Andreopoulos Y 2012 The performance of a self-excited fluidic energy harvester *Smart Mater. Struct.* 21 25007.
- [19] Dai H L, Abdelkefi A and Wang L 2014 Piezoelectric energy harvesting from concurrent vortex-induced vibrations and base excitations *Nonlinear Dyn.* 77 967–81.
- [20] Zhang L B, Dai H L, Abdelkefi A and Wang L 2017 Improving the performance of

aeroelastic energy harvesters by an interference cylinder Appl. Phys. Lett. 111 73904.

[21] Song J, Hu G, Tse K T, Li S W and Kwok K C S 2017 Performance of a circular cylinder piezoelectric wind energy harvester fitted with a splitter plate Appl. Phys. Lett. 111 223903.

[22] B. Seyed-Aghazadeh, D. Carlson and Y. Modarres-Sadeghi, "The influence of taper ratio on vortex-induced vibration of tapered cylinders in the crossflow direction", Journal of Fluids and Structures, vol. 53, pp. 84-95, 2015. Available: [10.1016/j.jfluidstructs.2014.07.014](https://doi.org/10.1016/j.jfluidstructs.2014.07.014).

APPENDIX I: ENGINEERING DATABASE

Gases

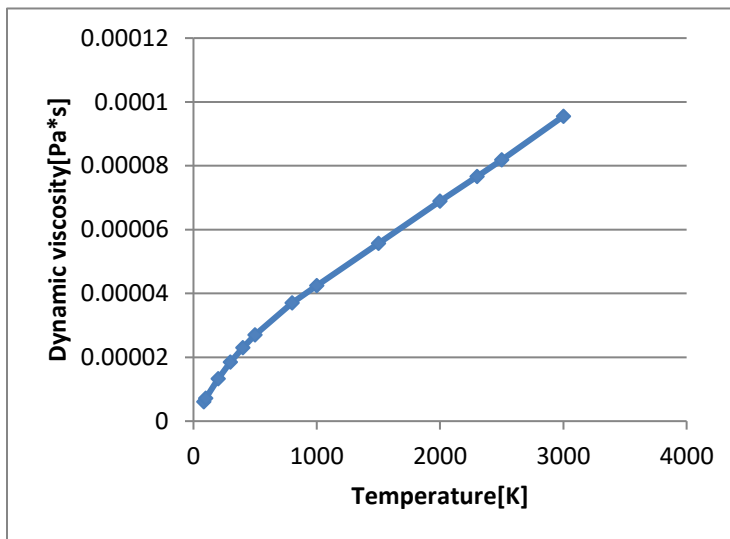
Air

Path: Gases Pre-Defined

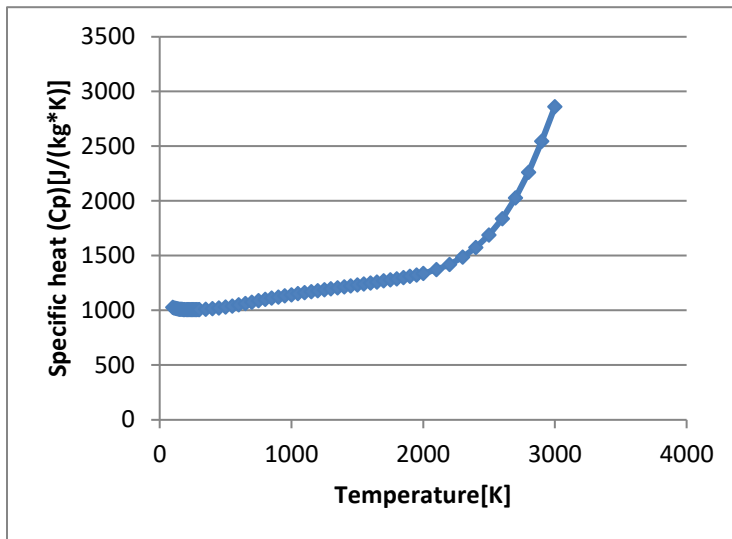
Specific heat ratio (C_p/C_v): 1.399

Molecular mass: 0.0290 kg/mol

Dynamic viscosity



Specific heat (Cp)



Thermal conductivity

